Synthetic, Structural, Spectroscopic, and Theoretical Studies of Decamethylvanadocene Arylnitrenes

Joseph H. Osborne,[1a] Arnold L. Rheingold,*[1b] and William C. Trogler*[1a]

Contribution from the Departments of Chemistry, D-006, University of California—San Diego, La Jolla, California 92093, and University of Delaware, Newark, Delaware 19716.
Received May 22, 1985

Abstract: The reaction between Cp^*_2V [$Cp^* = \eta$-$C_5(CH_3)_5$] and N_3R (R = 2,6-$(CH_3)_2C_6H_3$, C_6H_5, 2-$(C_6H_5)C_6H_4$, and $Cp^*_2VN_3$ yields Cp^*_2VNR (I, II, III, and IV, respectively). When the bulky azides, R = $SiMe_3$, $SiPh_3$, and CPh_3, were employed in the reaction, $Cp^*_2VN_3$ was produced. Complexes I–IV are formally 19e V(IV) complexes and exhibit solution μ_{eff} = 1.56–1.79 μ_B consistent with the presence of one unpaired electron. These nitrene complexes display isotropic EPR spectra in solution at room temperature (g = 1.986–1.988, a_V = 4.6–9.8, a_N = 4.6–4.9 × 10^{-4} cm^{-1}). The vanadium hyperfine splitting is ~1/10 that in typical V(IV) complexes, suggesting covalent V–N bonding. Crystals of I belong to the space group $P\bar{1}$, Z = 2, a = 8.584 (2) Å, b = 9.607 (3) Å, c = 15.899 (4) Å, α = 93.67 (3)°, β = 95.18 (3)°, and γ = 110.17 (4)°. Of the 2989 unique reflections collected, 2541 with $F_o > 2.5\sigma(F_o)$ were used in the solution and refinement of the structure, R_F = 0.0642, R_{wF} = 0.0794, and GOF = 2.034. The structure exhibits a linear V–N–C fragment [179.7 (5)°], short V–N bond [1.707 (6) Å], and small Cp (centroid)–V–Cp (centroid) angle [135.8 (3)°]. For the model complex $Cp_2VN(C_6H_5)$, SCF–Xα–DV calculations show two strong V–N π bonds in addition to the σ bond. Spin-polarized SCF–Xα–DV calculations predict an a_V/a_N ratio in close agreement with the experimental ratio. The calculated highest occupied molecular orbital is nonbonding and localized on V with an exchange splitting of 1.52 eV. Cyclic voltammograms of complexes I–IV in CH_2Cl_2 show quasi-reversible oxidations to 18e vanadium(V) complexes at potentials ~750 mV more negative than ferrocene.

Studies of metal oxo complexes have led to the development of reagents and catalysts for selective oxidations of organic substrates.[2] Isoelectronic metal–nitrene or imido complexes have received less attention[3] but may prove useful for transferring N–R groups to organic molecules.[3b] Most examples of metal–nitrene complexes[2] have been of high oxidation state coordination complexes. Properties of organometallic nitrenes[3d] need further definition. Our group has been interested[4] in the properties of unsaturated metal–nitrogen complexes. The report[5] that vanadocene forms stable nitrenes $Cp_2V(NSiMe_3)$ and $Cp_2V(NSiPh_3)$, where Cp = η-C_5H_5, Me = CH_3, and Ph = C_6H_5, prompted us to examine reactions between decamethylvanadocene and organic azides. While our study was in progress, the preparation and structure of $Cp^*_2V(NPh)$, where $Cp^* = \eta$-C_5Me_5, was communicated[6] in preliminary form. Although these nitrene complexes should be paramagnetic 19e systems, their magnetic and redox properties were not mentioned.[5,6] Herein we report syntheses of a family of arylnitrenes of decamethylvanadocene, structural studies of the 2,6-dimethylphenyl derivative, spin-polarized theoretical calculations, electrochemical oxidations, and EPR spectroscopic studies.

Experimental Section

Reactions were performed with standard Schlenk and cannula filtration techniques using a nitrogen atmosphere. Solids were manipulated under nitrogen in a Vacuum Atmospheres glovebox equipped with an HE-493 dri train. Glassware was oven-dried (180 °C) before use. Hydrocarbon and ether solvents were refluxed over sodium benzophenone ketyl and distilled under nitrogen. Methylene chloride was refluxed over CaH_2 for 24 h and distilled under nitrogen. Phenyl,[7a] pentafluorophenyl,[7a] xylyl,[7b] *o*-biphenyl,[7c] triphenylsilyl,[7d] and triphenylmethyl[7d] azides and $N_2{}^{15}NPh$[7e] were prepared by literature procedures.[7] (*Caution: some organic azides are explosive; exposure to acid or heavy metals should be avoided.*) The hazardous phenyl and xylyl azides were stored and used as 2.5–3.5 M benzene solutions. Trimethylsilyl azide (Aldrich Chemicals) was dried over 4-Å molecular sieves and degassed with an N_2 purge before use. The Cp*H and Cp^*_2V reagents were synthesized according to literature[8,9] methods. Sodium pentamethylcyclopentadienide was prepared by treating Cp*H with an equimolar amount of $NaNH_2$ in THF solvent. Following filtration, removal of the solvent in vacuo affords pale-yellow crystals of NaCp* (70% yield) that were washed with several portions of ether and used without further purification.

Bulk magnetic susceptibilities were measured by the Evans[10] NMR method with a Varian EM 390 spectrometer. EPR spectra were recorded with a Varian E-3 spectrometer, using external diphenylpicrylhydrazyl as the field marker, and IR spectra were recorded of Nujol mulls with a Perkin-Elmer 1330 spectrometer or an IBM IR32 FTIR spectrometer. Elemental analyses were performed by Galbraith Labs, Inc., or Schwarzkopf Microanalytical Laboratories.

Cyclic voltammograms were recorded with an IBM EC/225 polarographic/voltammetric analyzer and 7424MT x–y–t recorder. Solutions (CH_2Cl_2) were ca. 2 mM in the metal complex and contained 0.1 M tetrabutylammonium perchlorate (Baker electrochemical grade) sup-

(1) (a) University of California. (b) University of Delaware.

(2) (a) Sheldon, R. A.; Kochi, J. K. "Metal-Catalyzed Oxidations of Organic Compounds"; Academic Press: New York, 1981. (b) Alper, H. In "Transition Metal Organometallics in Organic Synthesis"; Academic Press: New York, 1978; pp 121–163. Hentges, S. G.; Sharpless, K. B. *J. Am. Chem. Soc.* **1980**, *102*, 4263–4265.

(3) (a) Nugent, W. A.; Haymore, B. L. *Coord. Chem. Rev.* **1980**, *31*, 123–175. (b) Chong, A. O.; Oshima, K.; Sharpless, K. B. *J. Am. Chem. Soc.* **1977**, *99*, 3420–3426. (c) Dehnicke, K.; Strähle, J. *Angew. Chem., Int. Ed. Engl.* **1981**, *20*, 413–486. (d) Fjare, D. E.; Gladfelter, W. L. *J. Am. Chem. Soc.* **1981**, *103*, 1572–1574.

(4) Gross, M. E.; Johnson, C. E.; Maroney, M. J.; Trogler, W. C. *Inorg. Chem.* **1984**, *23*, 2968–2973. Maroney, M. J.; Trogler, W. C. *J. Am. Chem. Soc.* **1984**, *106*, 4144–4151. Gross, M. E.; Trogler, W. C.; Ibers, J. A. *Organometallics* **1982**, *1*, 732–739. Gross, M. E.; Ibers, J. A.; Trogler, W. C. *Ibid.* **1982**, *1*, 530–535. Shi, Q.-Z.; Richmond, T. G.; Trogler, W. C.; Basolo, F. *Ibid.* **1982**, *1*, 1033–1037. Trogler, W. C.; Johnson, C. E.; Ellis, D. E. *Inorg. Chem.* **1981**, *20*, 980–986. Chang, C. Y.; Johnson, C. E.; Richmond, T. G.; Chen, Y. T.; Trogler, W. C.; Basolo, F. *Ibid.* **1981**, *20*, 3167–3172. Gross, M. E.; Ibers, J. A.; Trogler, W. C. *J. Am. Chem. Soc.* **1981**, *103*, 192–193. Gross, M. E.; Trogler, W. C. *J. Organomet. Chem.* **1981**, *209*, 407–414. Johnson, C. E.; Trogler, W. C. *J. Am. Chem. Soc.* **1981**, *103*, 6352–6358. Johnson, C. E.; Trogler, W. C. *Inorg. Chem.* **1982**, *21*, 427–429.

(5) Wiberg, N.; Häring, H.-W.; Schubert, U. *Z. Naurforsch. B* **1980**, *35b*, 599–603.

(6) Gambarotta, S.; Chiesi-Villa, A.; Guastini, C. *J. Organomet. Chem.* **1984**, *270*, C49–52.

(7) (a) Lindsay, R. O.; Allen, C. F. H. "Organic Syntheses"; Wiley: New York, 1955; Collect. Vol. 3, 710–711. (b) von E. Döering, W.; Odom, R. A. *Tetrahedron* **1966**, *22*, 81–86. Ugi, I.; Perlinger, H.; Behringer, L. *Chem. Ber.* **1958**, *91*, 2330–2336. (c) Smith, P. A. S.; Brown, B. B. *J. Am. Chem. Soc.* **1951**, *73*, 2438–2441. (d) Thayer, J. S.; West, R. *Inorg. Chem.* **1964**, *3*, 406–409. (e) Hillhouse, G. L.; Bercaw, J. E. *Organometallics* **1982**, *1*, 1025–1029.

(8) Manriquez, J. M.; Fagan, P. J.; Schertz, L. D.; Marks, T. J. *Inorg. Synth.* **1982**, *21*, 181–185.

(9) Robbins, J. L.; Edelstein, N.; Spencer, B.; Smart, J. C. *J. Am. Chem. Soc.* **1982**, *104*, 1882–1893.

(10) Evans, D. F. *J. Chem. Soc.* **1959**, 2003–2005.

0002-7863/85/1507-7945$01.50/0

porting electrolyte. For these measurements, a conventional three-electrode cell (Pt button working electrode, Pt-wire auxiliary electrode, Ag/Ag^+ –0.1 M $AgNO_3$ in CH_3CN reference electrode) was employed. Instrumental IR compensation was adjusted so that $E_{p_c} - E_{p_a}$ of the ferrocene/ferrocenium couple was 105 mV at a 200 mV/s scan rate.[11] The $E^{\circ\prime}$ value for the Cp_2Fe/Cp_2Fe^+ couple was 0.063 V in this cell.

Synthesis of 2,6-Dimethylphenylimidobis(pentamethylcyclopentadienyl)vanadium(IV), (η-$C_5Me_5)_2VN(2,6$-$Me_2C_6H_3$) (I). To a stirred solution of 0.32 g (1.0 mmol) of Cp^*_2V in 30 mL of ether was added 0.55 mL of a 2.7 M solution of 2,6-dimethylphenyl azide (1.5 mmol). The red solution became opaque and gradually turned green over 4.5 h. Solvents and excess azide were removed with a dynamic vacuum (liquid N_2 trap) for 12 h. The dark-green residue was dissolved in pentane and filtered, and its volume was reduced and the solution was cooled to afford dark-green air-sensitive needles of I (0.17 g, 39% yield): IR (mull) 1293 (m, C–N), 940 cm^{-1} (m, V–N). Anal. Calcd for $C_{28}H_{39}NV$: C, 76.27; H, 8.92. Found: C, 75.82; H, 9.00.

Synthesis of Phenylimidobis(pentamethylcyclopentadienyl)vanadium(IV), (η-$C_5Me_5)_2VN(C_6H_5)$ (II). This compound was prepared analogously to the 2,6-dimethylphenyl derivative. The reaction occurs rapidly, with vigorous evolution of N_2, and is complete within 2 h. From 0.85 g (2.65 mmol) of Cp^*_2V and 1.75 mL (3.5 M solution, 6.13 mmol) of phenyl azide, 0.69 g (1.67 mmol, 63% yield) of air-sensitive II was obtained. The complex is less stable than I, decomposing slowly in the solid state and within a day in solution: IR (mull) 1330 (m, C–N), 934 cm^{-1} (m, V–N). Anal. Calcd for $C_{26}H_{35}NV$: C, 75.76; H, 8.50; N, 3.40. Found: C, 73.59; H, 8.18; N, 3.02. The ^{15}N derivative $Cp^*_2V^{15}NPh$ was prepared in a similar fashion except the azide/Cp^*_2V ratio was 1.5:1: IR (mull) 1307 (m, C–^{15}N), 923 cm^{-1} (m, V–^{15}N).

Synthesis of 2-Biphenylimidobis(pentamethylcyclopentadienyl)vanadium(IV), (η-$C_5Me_5)_2VN(2$-$(C_6H_5)C_6H_4)$ (III). Dry ether (25 mL) was added to a solid mixture of Cp^*_2V (0.40 g, 1.25 mmol) and *o*-azidobiphenyl (0.25 g, 1.28 mmol). The red solution gradually becomes dark purple while stirring for 7 h. The volatile components were removed in vacuo, and the residue was dissolved in 75 mL of pentane and filtered. Reducing the solution volume, and cooling, produced air-sensitive dark blue–purple crystals of III in 49% yield (0.30 g): IR (mull) 1314 (m, C–N), 937 cm^{-1} (m, V–N). Anal. Calcd for $C_{32}H_{39}NV$: C, 78.66; H, 8.05. Found: C, 78.04; H, 8.44.

Synthesis of Pentafluorophenylimidobis(pentamethylcyclopentadienyl)vanadium(IV), (η-$C_5Me_5)_2VN(C_6F_5)$ (IV). To a stirring solution of 0.32 g of Cp^*_2V (1 mmol) in 15 mL of Et_2O was added 1.8 mmol of $N_3C_6F_5$ dissolved in 2 mL of toluene. The solution immediately turned green and gas was evolved. After further stirring for 1.5 h, the solution was reduced to dryness under vacuum. The residue was recrystallized from Et_2O to yield 0.35 g (70% yield) of IV: IR (mull) 1303 (m, C–N), 968 cm^{-1} (m, V–N). Anal. Calcd for $C_{26}H_{30}F_5NV$: C, 62.15; H, 6.02. Found: C, 61.69; H, 6.18.

Synthesis of Azidobis(pentamethylcyclopentadienyl)vanadium(III), (η-$C_5Me_5)_2VN_3$ (V). To 0.40 g (1.25 mmol) of Cp^*_2V in 25 mL of Et_2O, 0.45 mL of trimethylsilyl azide (3.51 mmol) was added by syringe. The red solution became blue–green with no apparent evolution of N_2. After stirring for 10 h, the volatiles were removed in vacuo, and the blue–green microcrystalline residue was dissolved in warm pentane and filtered. Cooling the solution yields V as blue cubic crystals in 42% yield (0.19 g): IR (mull) 2065 cm^{-1} (s, N=N=N). Anal. Calcd for $C_{20}H_{30}N_3V$: C, 66.10; H, 8.32; N, 11.56. Found: C, 66.22; H, 7.85; N, 11.20. Complex V also formed in the reactions between Cp^*_2V and N_3SiPh_3 or N_3CPh_3. Equimolar quantities of Cp^*_2V and the organic azide were mixed, and 30 mL of dry Et_2O was added. After stirring for 10 h, the solutions were reduced to dryness in pentane, dissolved, and filtered. Cooling yielded a mixture of blue cubic crystals and pale-yellow crystals. For the case of N_3CPh_3, Pasteur separation and IR analysis (comparison with authentic samples) proved the blue crystals to be compound V and the pale-yellow crystals were Ph_3CCPh_3.

Theoretical Studies. Electronic structure calculations were performed with a DEC-VAX 11/750 minicomputer and used the self-consistent field discrete variational Xα (SCF–DV–Xα) method.[12] Numerical atomic orbitals from exact Hartree–Fock–Slater calculations were used as basis functions, assuming the α values of Schwartz.[13] For V, the atomic orbitals through 4p were included. For C and N, a minimal 1s, 2s, 2p basis was used. For H, a 1s function was used. Core orbitals (1s, ..., 3p for V, and 1s for C and O) were frozen and orthogonalized against valence orbitals. The Mulliken[14] scheme was used to compute atomic orbital populations. The molecular Coulomb potential was calculated by using a least-squares fit[12] of the model electron density to the true density. Seven radial degrees of freedom were allowed in the expansion of the density, in addition to the radial atomic densities. For the molecular exchange potential, we set $\alpha = 0.716$. Spin-restricted SCF–DV–Xα calculations were performed to deduce qualitative bonding features. Spin-polarized SCF–DV–Xα calculations[15] were necessary to model the EPR spectra for the 19e nitrenes. As a computationally accessible model for the nitrene complexes, we used (η-$C_5H_5)_2VN(C_6H_5)$ with the experimental structure of I (vide infra) idealized to C_{2v} symmetry. Hydrogen atoms replaced the methyl groups of I on the Cp rings with an assumed C–H bond length of 1.08 Å.

Isotropic EPR hyperfine splittings of the V and N nuclei were estimated by the following procedures: (1) the valence molecular orbital and spin occupations for V and N were used to calculate spin-polarized atoms and allow core polarization; (2) the numerical value of the spin density at the nucleus was computed; (3) the Fermi contact hyperfine splitting was calculated with the expression $a_0 = (8\pi/3h)g_N\beta_N g\beta|\psi(0)|^2$. Parameters were obtained from an experimental spectrum by fitting the observed EPR spectrum to an effective spin Hamiltonian using the program[16] SIM14. This program was modified to allow calculation of isotropic spectra by adding a field dependency[17] to the line width.

Table I. Experimental Data for X-ray Diffraction Study of (η-$C_5Me_5)_2VN(2,6$-$Me_2C_6H_3)$

(A) Crystal Parameters at 23 °C	
crystal system: triclinic	V = 1219.3 (7) Å^3
space group: $P\bar{1}$	Z = 2
a = 8.584 (2) Å	M_r = 440.6 g/mol
b = 9.607 (3) Å	ρ(calcd) = 1.40 g cm^{-3}
c = 15.899 (4) Å	μ(Mo Kα) = 4.5 cm^{-1}
α = 93.67 (3)°	
β = 95.18 (3)°	
γ = 110.17 (3)°	

(B) Data Collection and Refinement

diffractometer: Nicolet R3
scan type: coupled θ(crystal) – 2θ(counter)
scan width: symmetrical, $[1.8 + \Delta(\alpha_2 - \alpha_1)]°$
scan speed: variable, 5–20°/min
reflns collected: $\pm h,\pm k,+l$; 2θ = 4–45°; 3225 total, 2989 unique, 2541 obsd ($F_o = 2.5\sigma(F_o)$)
crystal: green–black, 0.21 × 0.25 × 0.32 mm
standard reflections: 3 std/97 reflns (24% linear decay)
R_F, R_{wF}, GOF: 0.0642, 0.0794, 2.034
mean Δ/σ: 0.054
g = 0.001; $w^{-1} = \sigma^2(F_o) + gF_o^2$

X-ray Diffraction Study of I. A green–black crystal of I was affixed to a glass fiber and coated with epoxy cement to exclude the atmosphere. Unit cell parameters, provided in Table I, were obtained from angular settings of 25 reflections (21° ≤ 2θ ≤ 27°). Reflection data were processed with a profile-fitting scheme to improve the measurement of weak reflections, corrected for a 24% linear intensity decay and Lp effects but not for absorptions (uniform crystal dimensions, μ = 4.5 cm^{-1}, transmission variation <10.0%).

The vanadium atom position was obtained from a sharpened Patterson map; the remaining non-hydrogen atoms were located in subsequent difference Fourier syntheses. All non-hydrogen atoms were refined (block cascade methods) with anisotropic temperature factors, and the hydrogen atoms were placed in fixed, idealized locations (C–H = 0.96 Å, $U = 1.2U_{iso}$ of attached C atom) after locating at least one hydrogen in each methyl group to confirm rotational orientation; 272 total parameters were refined. The programs employed are contained in the SHELXTL library (version 4.1) distributed by the Nicolet Corp.

A diffusely contoured peak (2.13 e Å^{-3}) was found 1.81 Å from C(10), located remote from the Cp* rings, in the final difference Fourier map. We have no crystallographic explanation of this chemically meaningless peak. The next highest peak was 0.37 e Å^{-3}. The lowest trough was –0.39 e Å^{-3}. An analysis of variance showed no unusual trends with regard to the parity group, sin θ, Miller index, or $(E/E_{max})^{1/2}$.

(11) Gagné, R. R.; Koval, C. A.; Lisensky, G. C. *Inorg. Chem.* **1980**, *19*, 2854–2855. Gagné, R. R.; Allison, J. L.; Gall, R. S.; Koval, C. A. *J. Am. Chem. Soc.* **1977**, *99*, 7170–7178.
(12) Ellis, D. E.; Painter, G. S. *Phys. Rev. B* **1970**, *2*, 2887–2898. Delley, B.; Ellis, D. E. *J. Chem. Phys.* **1982**, *76*, 1949–1960.
(13) Schwartz, K. *Phys. Rev. B* **1972**, *5*, 2466.
(14) Mulliken, R. S. *J. Chem. Phys.* **1955**, *23*, 1833–1840.
(15) Delley, B.; Ellis, D. E.; Freeman, A. J.; Baerends, E. J.; Post, D. *Phys. Rev. B.* **1983**, *27*, 2132–2144.
(16) Lozos, G. P.; Hoffmann, B. M.; Franz, C. G. *QCPE* **1974**, *No. 11*, 265.
(17) Meyers, R. J. "Molecular Magnetism and Magnetic Resonance Spectroscopy"; Prentice-Hall: New Jersey, 1973.

Table II. Atom Coordinates ($\times 10^4$) and Temperature Factors ($Å^2 \times 10^3$)

atom	x	y	z	U_{iso}[a]
V	2681 (1)	2580 (1)	2698 (1)	31 (1)*
N	2590 (7)	3963 (6)	2094 (3)	35 (2)*
C(1)	3326 (8)	991 (7)	1737 (4)	38 (3)*
C(2)	1861 (9)	1174 (7)	1383 (4)	39 (3)*
C(3)	598 (8)	546 (7)	1902 (5)	43 (3)*
C(4)	1247 (9)	−166 (7)	2522 (4)	44 (3)*
C(5)	2913 (8)	82 (7)	2415 (4)	39 (3)*
C(6)	4966 (10)	1426 (9)	1372 (5)	61 (4)*
C(7)	1659 (10)	1870 (8)	574 (4)	55 (4)*
C(8)	−1195 (9)	401 (9)	1754 (6)	67 (4)*
C(9)	181 (11)	−1257 (9)	3067 (6)	75 (4)*
C(10)	4045 (11)	−659 (9)	2804 (5)	69 (4)*
C(11)	3327 (9)	2178 (8)	4185 (4)	44 (3)*
C(12)	4784 (9)	3178 (10)	3897 (4)	53 (3)*
C(13)	4449 (10)	4480 (8)	3737 (4)	57 (3)*
C(14)	2814 (11)	4276 (8)	3870 (4)	52 (3)*
C(15)	2099 (9)	2833 (8)	4122 (4)	43 (3)*
C(16)	3228 (12)	824 (9)	4635 (5)	72 (4)*
C(17)	6443 (11)	3011 (13)	3892 (6)	99 (6)*
C(18)	5719 (14)	5902 (11)	3531 (6)	116 (5)*
C(19)	1989 (15)	5427 (11)	3822 (6)	98 (6)*
C(20)	366 (11)	2198 (11)	4411 (6)	78 (5)*
C(21)	2525 (9)	5092 (7)	1606 (4)	39 (3)*
C(22)	1052 (9)	5408 (8)	1467 (5)	49 (3)*
C(23)	1022 (11)	6538 (9)	981 (5)	61 (4)*
C(24)	2402 (11)	7379 (9)	634 (5)	68 (4)*
C(25)	3834 (11)	7048 (8)	747 (5)	59 (4)*
C(26)	3957 (9)	5921 (7)	1226 (4)	42 (3)*
C(27)	5517 (10)	5582 (8)	1302 (5)	57 (3)*
C(28)	−522 (10)	4498 (10)	1807 (6)	69 (4)*

[a] * means equivalent isotropic U defined as one-third of the trace of the orthogonalized U_{ij} tensor.

Final positional parameters are listed in Table II; anisotropic thermal parameters, a complete table of bond distances and angles, hydrogen coordinates, and a table of observed and calculated structure factors are available as supplementary material.

Results and Discussion

Decamethylvanadocene and aryl azides react at room temperature to evolve nitrogen and produce nitrene complexes (eq 1). Solutions of these complexes hydrolyze slowly but react instantly with oxygen. The dark-green solutions of I–IV exhibit

$$Cp^*_2V + N_3Ar \rightarrow N_2 + Cp^*_2VNAr \quad (1)$$

$$\text{I, Ar} = 2,6\text{-}Me_2C_6H_3$$

$$\text{II, Ar} = C_6H_5$$

$$\text{III, Ar} = 2\text{-}(C_6H_5)C_6H_4$$

$$\text{IV, Ar} = C_6F_5$$

characteristic EPR spectra that show coupling to both the V and N atoms. All complexes show characteristic[18a] medium-intensity IR absorptions at 1290–1382 and 930–970 cm^{-1} attributable to the N–C and V–N stretches. Employing $N_2{}^{15}NC_6H_5$ in eq 1 yields II with complete incorporation of the ^{15}N label (by EPR and IR analyses). This supports the mechanism of eq 2 for nitrene formation, where the α nitrogen of the azide attacks the metal.

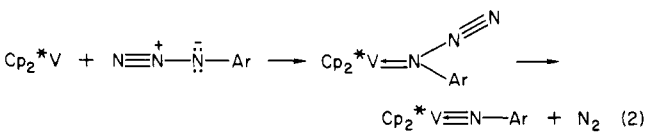

The proposed intermediate may be metastable since Gambarotta et al.[6] observed at 0 °C an insoluble brown complex from the

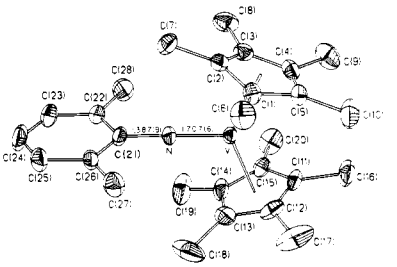

Figure 1. Molecular structure and atom labeling scheme for $(\eta\text{-}C_5Me_5)_2VN[2,6\text{-}Me_2C_6H_3]$ drawn with 40% thermal ellipsoids.

Table III. Selected Bond Distances and Angles for $(\eta\text{-}C_5Me_5)_2VN(2,6\text{-}Me_2C_6H_3)$

	(A) Bond Distances, Å		
V–N	1.707 (6)	V–CNT1[a]	2.073 (6)
N–C(21)	1.387 (9)	V–CNT2[a]	2.075 (6)
	(B) Bond Angles, deg		
CNT1–V–CNT2[a]	135.8 (3)	V–N–C (21)	179.7 (5)
CNT1–V–N[a]	112.7 (3)		
CNT2–V–N[a]	111.5 (3)		

[a] CNT = centroid of Cp*.

reaction between Cp^*_2V and N_3Ph, that on warming evolved N_2 to yield II. Azide exchange (eq 3) does not occur at room tem-

$$Cp^*_2V{\equiv}{}^{15}N{-}Ph + N_3Ph \rightarrow Cp^*_2V{\equiv}N{-}Ph + N_2{}^{15}NPh \quad (3)$$

perature (4 h) as evidenced by the retention of ^{15}N hyperfine splitting in the EPR spectrum of $Cp^*_2V^{15}NPh$ when a tenfold excess of N_3Ph was added.

Addition of hindered azides to Cp^*_2V yielded a V(III) azido complex, eq 4, that exhibits a strong absorption at 2065 cm^{-1} in the IR spectrum characteristic[18b] of terminally bound azide ion.

$$Cp^*_2V + N_3R \rightarrow Cp^*_2VN_3 + {}^1/_2R_2 \quad (4)$$

$$R = CPh_3,\ SiMe_3,\ SiPh_3$$

This is to be contrasted with the reactivity of vanadocene,[5] eq 5, or the reaction between vanadocene and HN_3 that yields[19] shock-sensitive $Cp_2V(N_3)_2$. Because of steric considerations, we

$$Cp_2V + N_3SiPh_3 \rightarrow Cp_2VNSiPh_3 + N_2 \quad (5)$$

favor a mechanism for reaction 4 where N_3R approaches the metal with the γ nitrogen, and azide abstraction occurs. The one-electron-reducing properties of vanadocene are further illustrated by formation of the μ-isocarbonyl complex $Cp^*_2VOCV(CO)_5$ from the reaction[20] between Cp^*_2V and $V(CO)_6$.

Reactions between Cp_2V and phenyl, 2,6-dimethylphenyl, or cyclohexyl azide yield red, unstable, EPR active oils. Reactions between Cp^*_2V and cyclohexyl or methyl azide yielded red oils whose EPR spectra were not readily interpreted.

Molecular Structure of $[\eta\text{-}C_5(CH_3)_5]_2V[N\text{-}2,6\text{-}(CH_3)_2C_6H_3]$. The structure of I (Figure 1) is similar to that reported[6] recently for II. The V–N–C unit is linear (Table III) with a bond angle of 179.7 (5)°. For linear binding, we propose that the N–R group donates 4e to the metal (2σ and 2π) to yield a 19e complex. The short V–N bond length [1.707 (6) Å], as compared to related V–C distances in Cp^*_2VCO or Cp^*_2VCN (Table IV), are consistent with V–N multiple bonding. Most nitrene complexes with more than an 18e count exhibit bent M–N–R moieties.[3a] The linear bonding observed here is attributed to two strong V–N π bonds (vide infra), one of which would weaken if bending occurred. From formal considerations, we regard the NR moiety as a 2– unit and vanadium in the +IV oxidation state. In this context, compare the Cp*–V–Cp* angle in I to that in Cp^*_2VCO, V(II) or $(CpMe_2)VCl_2$, V(IV) (Table IV).

(18) (a) Osborne, J. H.; Trogler, W. C. *Inorg. Chem.* **1985**, *24*, 3098–3099. (b) Nakamoto, K. "Infrared and Raman Spectra of Inorganic and Coordination Compounds", 3rd. ed.; Wiley: New York, 1978.

(19) Moran, A.; Gayoso, M. *J. Organomet. Chem.* **1983**, *243*, 423–426.

(20) Osborne, J. H.; Rheingold, A. L.; Trogler, W. C. *J. Am. Chem. Soc.*, in press.

Table IV. Selected Bond Lengths and Angles[a] for Related Bent Metallocenes, Cp_2MX-Y

complex[b]	EAN	d^n	metal ox state	Cp–M–Cp angle[c]	M–X length	X–Y length	M–X–Y angle	Cp–M[c] length	ref
$Cp^*_2VN(2,6\text{-}Me_2C_6H_3)$	19	d^1	IV	135.8 (3)	1.707 (6)	1.387 (9)	179.7 (5)	2.074 (6)	this work
$Cp^*_2VN(C_6H_5)$	19	d^1	IV	138.4 (3)	1.730 (5)	1.345 (9)	178.2 (6)	⟨2.054⟩	*d*
$Cp_2VNSi(CH_3)_3$	19	d^1	IV	130.9 (8)	1.665	1.736	178.0 (6)	2.054	*e*
$Cp^*_2V-OC-V(CO)_5$	16	d^2	III	148.9 (2)	2.075 (4)	1.167 (6)	180.0	1.966 (5)	*f*
Cp^*_2VCO	17	d^3	II	153.6 (4)	1.879 (8)	1.17 (1)	178.1 (8)	⟨1.925⟩	*g*
Cp^*_2VCN	16	d^2	III	151.5 (3)	2.088 (7)	1.127 (8)	178.7 (6)	⟨1.97⟩	*g*
Cp_2VCl	16	d^2	III	139.5 (3)	2.390 (4)			⟨1.946⟩	*h*
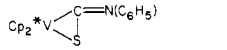	17	d^3	II	143.1 (3)				⟨2.007⟩	*i*
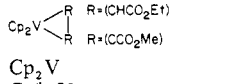	17	d^3	II	135.9 (5)				⟨1.956⟩	*j*
	17	d^3	II	138.4 (2)				⟨1.960⟩	*j*
Cp_2V	15	d^3	II	180				1.92	*k*
Cp^*_2V	15	d^3	II	180				⟨1.90⟩	*l*
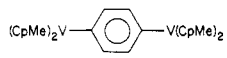	16	d^2	III	146.2	⟨2.14⟩			⟨1.965⟩	*m*
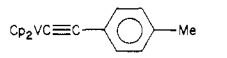	16	d^2	III	149.7 (1)	2.034 (13)		176.6 (10)	⟨1.973⟩	*n*
$(CpMe)_2VCl_2$	17	d^1	IV	133.4	2.398 (2)			1.991	*o*

[a] Standard deviations are given when values were reported. [b] $Cp=C_5H_5$, $Cp^*=C_5Me_5$, $CpMe=C_5H_4CH_3$. [c] Cp here refers to the centroid of either the C_5H_5, C_5H_4Me, or C_5Me_5 ring. Numbers in brackets are an average of two values. [d] Gambarotta, S.; Chiesi-Villa, A.; Guastini, C. *J. Organomet. Chem.* **1984**, *270*, C49–C52. [e] Wiberg, N.; Häring, N.-W.; Schubert, U. *Z. Naturforsch. B* **1980**, *35b*, 599–603. [f] Osborne, J. H.; Rheingold, A. L.; Trogler, W. C. *J. Am. Chem. Soc.*, in press. [g] Gambarotta, S.; Floriani, C.; Chiesi-Villa, A.; Guastini, C. *Inorg. Chem.* **1984**, *23*, 1739–1747. [h] Fieselmann, B. J.; Stucky, G. D. *J. Organomet. Chem.* **1977**, *137*, 43–54. [i] Gambarotta, S.; Fiallo, M. L.; Floriani, C.; Chiesi-Villa, A.; Guastini, C. *Inorg. Chem.* **1984**, *23*, 3532–3537. [j] Fachinetti, G.; Floriani, C.; Chiesi-Villa, A.; Guastini, C. *Inorg. Chem.* **1979**, *18*, 2282–2287. [k] Antipin, M. Yu.; Lobkovskii, E. B.; Semenenko, K. N.; Soloveichik, G. L.; Struchkov, Yu. T. *J. Struct. Chem.* (*Engl. Transl.*) **1979**, *20*, 810–816. [l] Reference g, crystal is disordered. [m] Köhler, F. H.; Prössdorf, W.; Schubert, U. *Inorg. Chem.* **1981**, *20*, 4096–4101. [n] Köhler, F. H.; Prössdorf, W.; Schubert, U.; Neugebauer, D. *Angew. Chem., Int. Ed. Engl.* **1978**, *17*, 850–851. [o] Peterson, J. L.; Dahl, L. F. *J. Am. Chem. Soc.* **1975**, *97*, 6422–6432.

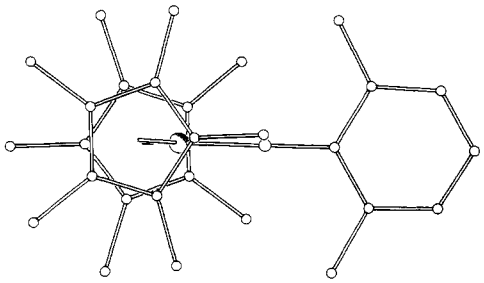

Figure 2. View of $(\eta\text{-}C_5Me_5)_2VN[2,6\text{-}Me_2C_6H_3]$ shown without perspective to emphasize the staggered orientation of the Cp* rings.

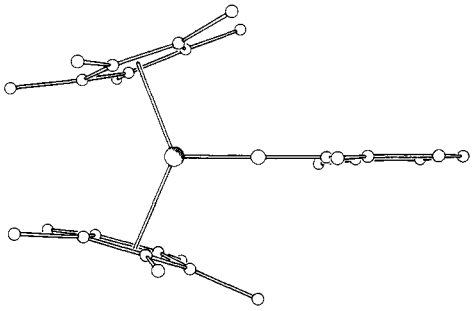

Figure 3. View of $(\eta\text{-}C_5Me_5)_2VN[2,6\text{-}Me_2C_6H_3]$ showing the relative orientations of the three planar ring systems.

As expected, the orientation of the two Cp* groups (Figure 2) is staggered to minimize nonbonded repulsions. The V–Cp*-(centroid) distance in I and II is 0.1 (Å) longer than usually observed in vanadium metallocenes (Table IV). This may be attributed to the high (19e) electron count and to steric crowding because of the small Cp*–V–Cp* angles (Table IV). Examination of individual V–C bond lengths shows that the three ring carbons pointed toward the nitrene ligand [V–C range 2.325 (5)–2.378 (7) Å] are closer to vanadium than those [V–C range 2.398 (7)–2.492 (8) Å] on the opposite side of the C_5 rings. While the Cp* methyl groups are deflected out of the plane, this is not significantly larger for the methyls in close contact between the rings as opposed to those oriented toward the nitrene ligand. The minimum contact between Cp* methyls is that between H(16b) and H(9a) = 2.019 Å. Rotation of the Cp* rings as a unit appears to occur to achieve maximum overlap with the metal orbitals while maintaining minimum steric repulsion between the Cp* rings and the "NR" ligand (shown below).

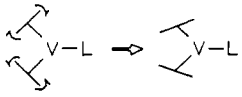

If the Cp* ligand is viewed as having its center of bonding located somewhat below the plane of the ring, then rotation about this center would produce the observed long V–Cp* centroid length and the variation in V–C distances.

Lauher and Hoffmann[21] have shown that the Cp–M–Cp angle in the Cp_2ML species is related to the σ- and π-bonding properties of the ligand. They conclude that a decreased Cp–M–Cp angle is a consequence of strong ligand π-acceptor character. A poor σ donor will also be associated with small values of this angle. The "NR" moiety is proposed[3] to be a strong π-acceptor ligand approaching the strength of the nitrido ligand. Representative bond angles and distances are shown in Table IV for I, II, and related compounds. The Cp–V–Cp angle may be seen to depend on the ligand and degree of alkylation of the Cp ring; the angle increases for the peralkylated complexes by ~5–7°. In the model of Lauher and Hoffmann,[21] the small Cp*–V–Cp* angles found in decamethylvanadocene nitrenes suggest strong π back bonding to the nitrene ligand. The orientation of the aryl substituent plane between the Cp* planes (Figure 3) will be considered with the MO calculations described below.

EPR Spectra, Xα Calculations, and Electrochemical Studies. Bulk magnetic susceptibility measurements yield μ_{eff} values (Table V) of 1.56–1.79 μ_B for the nitrene complexes. This is close to the spin-only value of 1.73 μ_B for a doublet ground state. By contrast, the V(III) complex $Cp^*_2VN_3$ exhibits a μ_{eff} of 2.70 μ_B that is

(21) Lauher, J. W.; Hoffmann, R. *J. Am. Chem. Soc.* **1976**, *98*, 1729–1742.

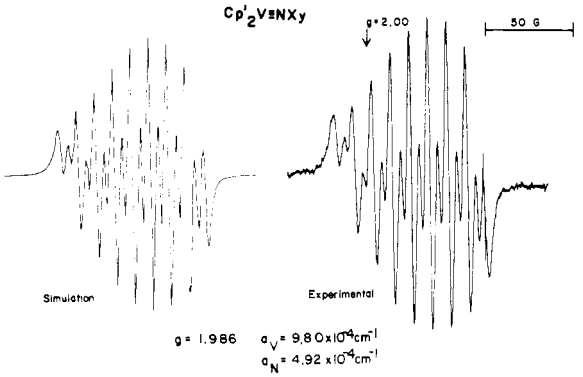

Figure 4. Observed and simulated solution EPR spectra of Cp^*_2VN-(2,6-$Me_2C_6H_3$).

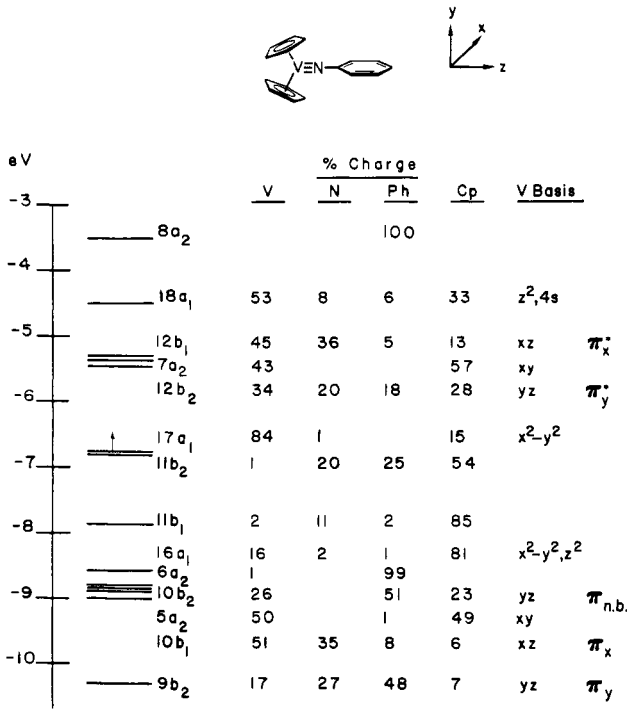

Figure 5. Orbital energy diagram and atomic compositions from SCF–Xα-DV calculations of Cp_2VNPh.

consistent with a triplet ground state. All the nitrene complexes display isotropic EPR spectra (g = 1.986–1.988) at room temperature in solution. For the Cp^*_2V derivatives, both vanadium (I = 7/2) and nitrogen I = 1) hyperfine splittings are resolved. Computer simulation using an effective spin Hamiltonian (Figure 4) yields the hyperfine splitting parameters of Table V. The proposed nitrogen hyperfine splitting in Cp^*_2VNPh was conclusively identified by observing the EPR spectrum of the ^{15}N-labeled complex.

The EPR spectra exhibit an unusually low vanadium hyperfine splitting. As a general trend, we note that a_V increases with the formal oxidation state from 25 G (1 G $\sim 10^{-4}$ cm^{-1}) in Cp^*_2V[9] to 60–75 G in Cp_2VX_2 or $Cp^*_2VX_2$ complexes[22] (where X = Cl, alkyl, and SCN). Acetylene derivatives of decamethylvanadocene exhibit[23] intermediate values of a_V (e.g., 43 G). Small a_V and large a_N values in the nitrene complexes might result from covalent V–N π bonding.

To further understand V–N bonding in these complexes, we performed SCF–Xα–DV calculations for the model complex Cp_2VNPh, whose geometry was idealized to C_{2v} symmetry (C_2 along V–N bond).[24] Upper valence orbitals and their charge distributions are shown for a spin-restricted calculation in Figure 5. A table of calculated energy levels and orbital charge dis-

Table V. EPR[a] and Magnetic Susceptibility[b] Data for Nitrene Complexes of Vanadocene and Decamethylvanadocene as well as $Cp^*_2VN_3$

compound	g_{iso}	a_V, 10^{-4} cm^{-1}	a_N, 10^{-4} cm^{-1}	μ_{eff}, μ_B
Cp^*_2VNPh	1.988	9.34	4.68	1.56
$Cp^*_2V^{15}NPh$	1.988	9.34	9.28	
$Cp^*_2VNC_6F_5$	1.988	4.6	4.6	1.79
$Cp^*_2VN(2,6\text{-}Me_2C_6H_3)$	1.986	9.80	4.92	1.68
$Cp^*_2VN[2\text{-}(C_6H_5)C_6H_4]$	1.988	6.25	4.64	1.58
$Cp_2VNSiPh_3$	1.987	c	c	1.66
"Cp_2VNPh"	1.990	~30[d]	c	
"$Cp_2VN(2,6\text{-}Me_2C_6H_3)$"	1.987	~40[d]	c	
$Cp^*_2VN_3$	1.988	69.6		2.70

[a] Room temperature ~0.5 mM solutions in toluene or CH_2Cl_2. [b] Determined at room temperature by the Evans method using CH_2Cl_2 solvent. [c] Not resolved. [d] Complex 16 line spectrum of reaction solution.

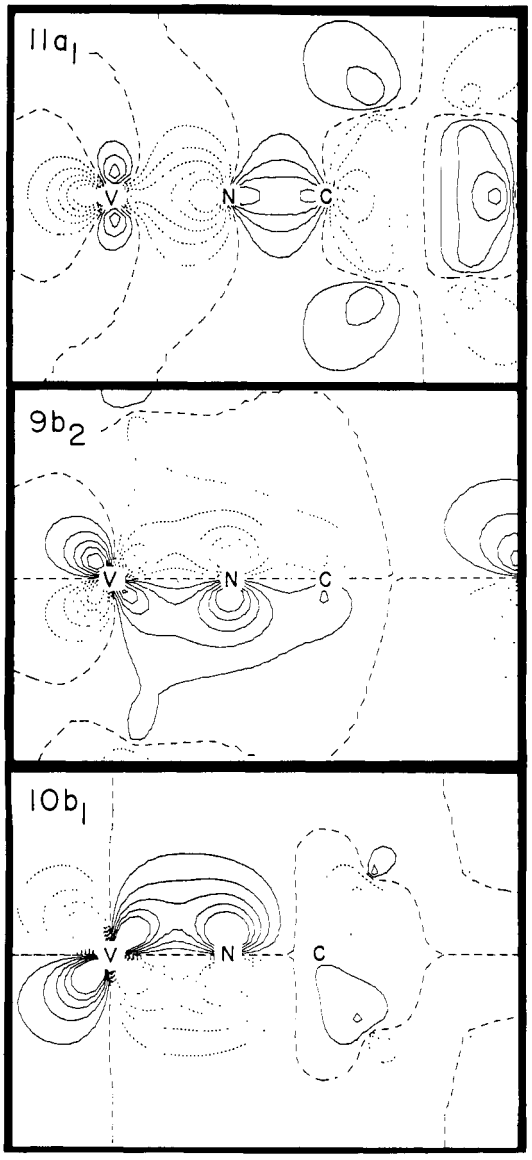

Figure 6. Contour plots of (a, top) the σ-bonding $11a_1$ orbital, (b, middle) the π-bonding $9b_2$ orbital, and (c, bottom) the π-bonding $10b_1$ orbital. The contour interval in this and Figure 7 is 0.270 e/Å^3.

(22) Connelly, N. G. In "Comprehensive Organometallic Chemistry"; Wikinson, G. Stone, F. G. A., Abel, E. W., Eds.; Pergamon Press: Oxford, 1982; Vol. 3, pp 647–704 and references therein.

(23) Petersen, J. L.; Griffith, L. *Inorg. Chem.* **1980**, *19*, 1852–1858.

(24) Note that our coordinate system differs from that of ref 21 in the choice of x and y. The only effect is to interchange b_1 and b_2 symmetry labels.

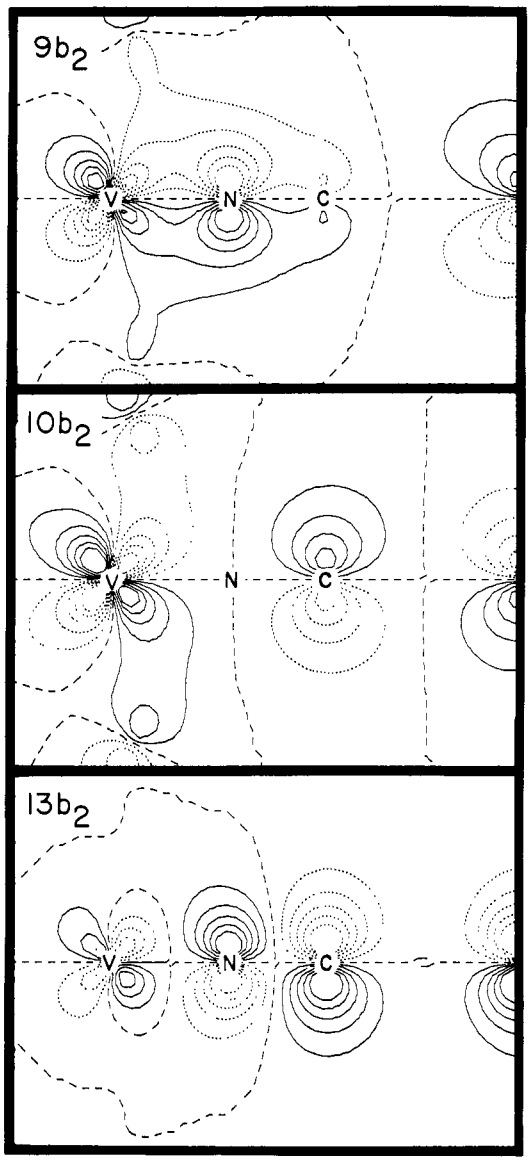

Figure 7. Contour plots of three-center π orbitals of Cp_2VNPh, (a, top) $9b_2$ (bonding), (b, middle) $10b_2$ (nonbonding), and (c, bottom) $13b_2$ (antibonding).

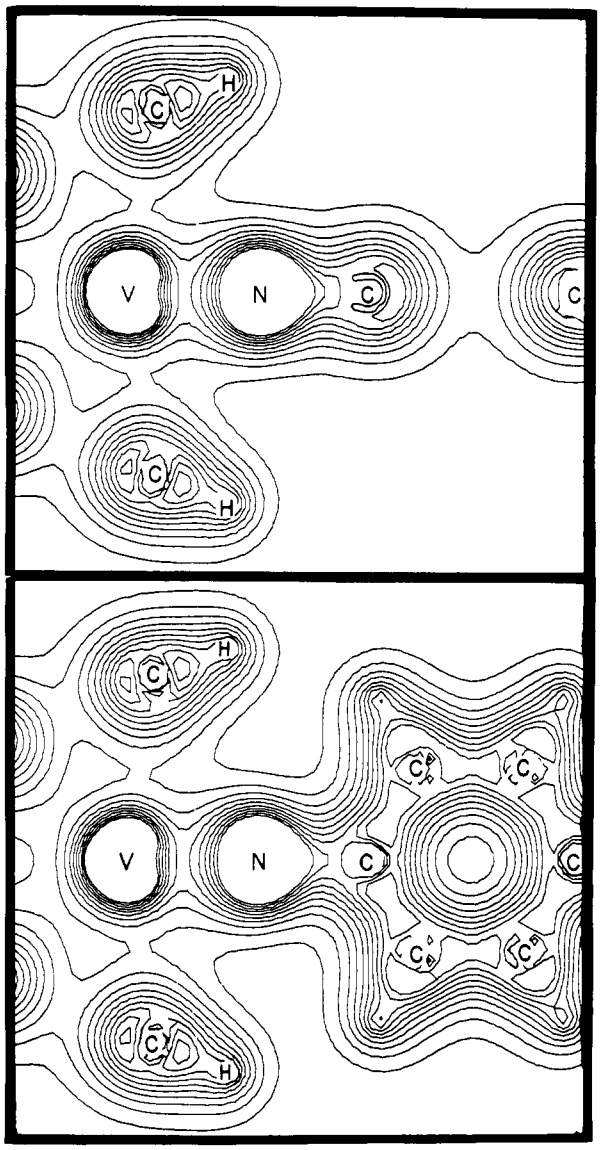

Figure 8. Contour plots of the total electron density for Cp_2VNPh for two N–Ph group orientations. The contour interval is 0.169 $e^2/Å^3$.

tributions for all valence orbitals (both spin-polarized and spin-restricted) is available as supplementary material. Except for the $11a_1$ level, the lower valence orbitals (not shown in Figure 5) are of cyclopentadienyl or phenyl character (the C–H and C–C bonding interactions). Consistent with the structure, the calculation shows strong covalent bonding between vanadium and nitrogen. The $11a_1$ orbital located at −12.8 eV, (19%, 20%, and 46% vanadium, nitrogen, and phenyl carbon character, respectively) is identified as the V–N σ bond. This orbital, shown in Figure 6a, exhibits three-center bonding over the V–N–C fragment and is composed of Vd_{z^2}, Np_z, and a phenyl p–σ orbital. The two π-bonding V–N interactions are shown in Figure 6b (perpendicular to the C_6H_5 plane) and 6c (parallel to the C_6H_5 plane). The $9b_2$ orbital is stabilized relative to $10b_1$ by a small interaction with Cp pπ orbitals. Nitrogen–carbon π bonding occurs primarily in the $7b_2$ orbital and is weak.

The presence of the strong π-bonding $9b_2$ orbital suggests that the Cp_2V b_2 orbital is energetically accessible in contrast to previous results[21] of extended Hückel calculations for Cp_2M fragments. This orbital is required to form the triple bond between vanadium and nitrogen. The $9b_2$ orbital is the bonding component of a three-center, four-electron bond (Figure 7), with the $10b_2$ and $13b_2$ orbitals being the nonbonding and antibonding components, respectively.

The HOMO is calculated to be of $17a_1$ symmetry and essentially pure $V(d_{x^2-y^2})$; however, 0.04 eV separates this orbital from the filled $11b_2$ level, a Cp-localized orbital.

The relative orientation of the phenyl plane to the bent Cp_2M fragment in Cp_2VPh and Cp_2VC_2Ph has been considered by Köhler, Hofmann, and Prössdorf.[25] They find that the highest occupied level is a metal-localized a_1 orbital consistent with the results found here. When C_6H_5 is bound to the metal via an ethynyl (C_2) group, the conformation where the phenyl plane is oriented to maximize conjugation with the b_1 π orbital (b_2, in the other coordinate system[24]), A, is favored slightly over the configuration B observed in the solid state.

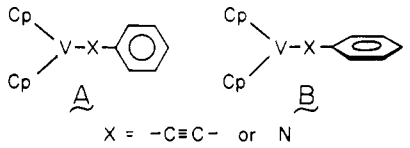

Calculations of Cp_2VNPh in conformers A and B show only minor differences in energies of the individual levels and in contour

(25) Köhler, F. H.; Hofmann, P.; Prossdorf, W. *J. Am. Chem. Soc.* **1981**, *103*, 6359–6357.

Table VI. Calculated[a] Spin Distribution in $Cp_2VN(C_6H_5)$

atom	orbital	occupation	spin density	orbital (spin density at nucleus[b])
V	3d	4.630	1.949	1s (−0.006), 2s (−0.393)
	4s	0.228	0.079	3s (+0.022), 4s (+0.282)
	4p	1.053	0.002	total (−0.0969)
N	2s	1.565	−0.033	1s (0.149), 2s (−0.332)
	2p	3.134	−0.661	total (−0.184)
$C(C_6)$	2s	1.553	0.001	
	2p	2.542	−0.011	
$H(C_6)$	1s	0.897	0.000	
$C(C_5)$	2s	1.462	0.001	
	2p	2.572	−0.033	
$H(C_5)$	1s	0.900	0.005	

[a] From spin-polarized calculations. [b] By using molecular spin density to perform an atomic spin-polarized calculation that allows for core polarization. The occupation number of a spin-up atomic orbital times the spin-down orbital density at the nucleus minus the occupation number of a spin down atomic orbital times the spin-down orbital density at the nucleus yields the orbital contribution to the spin density at the nucleus.

Table VII. Electrochemical Data for Decamethylvanadocene Nitrenes from Cyclic Voltammetry[a]

compound	$E^{0\prime}$,[b] V	i_{pa}/i_{pc}	ΔE_p, V
Cp^*_2VNPh	−0.663	1.32	0.050
$Cp^*_2VNC_6F_5$	−0.390	1.49	0.035
$Cp^*_2VN(2,6\text{-}Me_2C_6H_3)$	−0.677	1.08	0.098
$Cp^*_2VN[2\text{-}(C_6H_5)C_6H_4]$	−0.680	1.10	0.090
Cp_2Fe	+0.083	1.01	0.105

[a] Recorded at 200 mV/s in 2 mM CH_2Cl_2 solutions containing 0.1 M tetrabutylammonium perchlorate and referenced to an Ag/0.1 M $AgNO_3$ in CH_3CN electrode. [b] $(E_{pa} - E_{pc})/2$ for oxidation of parent compound.

plots for the bonding orbitals. One concludes that the V–N bond is equally strong in both conformers from the total density contours (Figure 8); however, the N–C σ bond appears slightly stronger and there is more electron density delocalized onto the phenyl ring in conformer A. Since conformer A is expected to be slightly more stable than B (because of more favorable π conjugation between V–N b_1 and Ph π orbitals), we attribute the existence of structure B in crystals of II to packing forces.

Total electron density plots of the two rotomers (Figure 8) illustrate the accessibility of V to attack by electrophiles in conformer A and the sterically protected environment in structure B. The plots also suggest that steric effects in Cp^*_2VN (2,6-dimethylphenyl) and Cp^*_2VN(2-biphenyl) should favor conformer B. This may account for the solution stability of I and III in contrast to that of II, which even decomposes slowly in hydrocarbon solvents. A similar explanation accounts for the instability of Cp_2V nitrene analogues except for those[5] with very bulky nitrene substituents (e.g., $SiPh_3$).

Spin-polarized calculations (available as supplementary tables) place the unpaired electron of Cp_2VNPh in a vanadium-localized $17a_1$ orbital. The nearly degenerate $11b_2$ orbital has significant nitrogen character but no vanadium component. The V and N hyperfine splitting observed in the EPR spectrum has no simple orbital interpretation. The calculated valence spin distribution (Table VI) in combination with atomic spin-polarized calculations (see Experimental Section) yields a_V = 40 G and a_N = 20 G for the contact hyperfine splittings. Although the calculated a_V/a_N ratio is in good agreement with the experimental ratio of 2.00, the magnitude of the calculated splittings is almost 4 times too large. The error may arise from uncertainties in the calculational procedure used to estimate spin density at the nucleus. Since Cp* is a basic ligand that interacts more strongly with V than Cp, this should also decrease the spin density at V and N. Recall (Figure 5) that the calculation showed a large Cp contribution to the highest occupied $17a_1$ and $11b_2$ orbitals. Although the Cp complexes could not be isolated, reaction mixtures from Cp_2V and phenyl azide or 2,6-dimethylphenyl azide exhibited EPR spectra (Table V) with a_V close to that calculated.

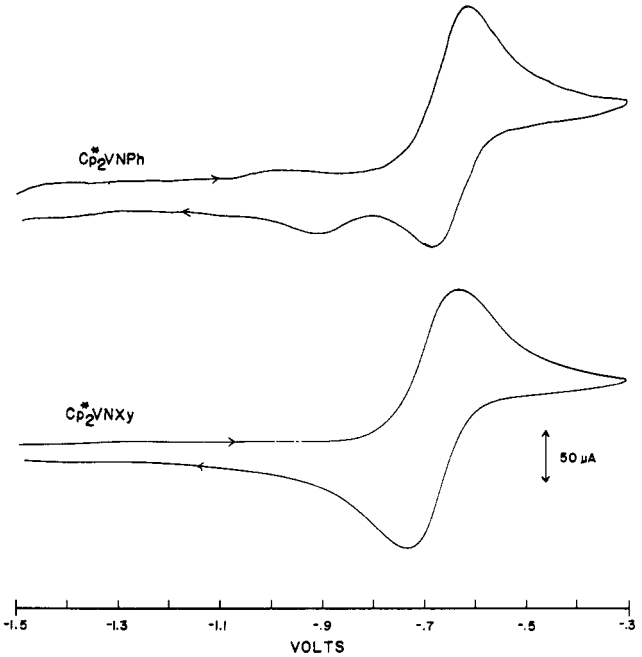

Figure 9. Cyclic voltammograms (200 mV/s) of Cp^*_2VNXy, where Xy = $2,6\text{-}Me_2C_6H_3$, and Cp^*_2VPh in CH_2Cl_2/0.1 M NBu_4ClO_4 vs. a Ag/0.1 M $AgNO_3$ (in CH_3CN) reference.

Table VIII. Volume-Integrated Atomic Charges[a] in $Cp_2VN(C_6H_5)$

atom	volume integrated charges: perpendicular[b]	volume integrated charges: parallel[c]	perpendicular (spin pol)
V	−0.369	−0.360	−0.361
N	−0.178	−0.211	−0.168
C(Ph)	+0.440	+0.437	+0.442
H(Ph)	−0.472	−0.475	−0.470
C(Cp)	+0.493	+0.491	+0.490
H(Cp)	−0.467	−0.459	−0.467

[a] Charge partitioned to an atom according to the region of space closest to that atom. [b] For the phenyl ring oriented in the *xz* plane, configuration B (see Figure 5). [c] For the phenyl ring oriented in the *yz* plane, configuration A.

When we considered the 19e configuration of decamethylvanadocene nitrenes and the nonbonding nature of the highest occupied $17a_1$ orbital, it seemed that the nitrenes should be susceptible to oxidation (eq 6). Characterization by cyclic voltammetry (Table VII, Figure 9) shows that the nitrene complexes

$$Cp^*_2VNR \xrightarrow{-e} Cp^*_2VNR^+ \quad (6)$$

oxidize more readily (ca. 0.75 V more negative) than ferrocene. The ratio of anodic and cathodic peak currents establish quasi-reversible behavior for the N(2,6-dimethylphenyl) and N(2-biphenyl) derivatives. The NPh derivative oxidizes irreversibly at scan rates up to 500 mV/s. We attribute the instability of the NPh species to the steric accessibility of the A rotomer (vide supra). Future work will be directed toward the reactivity of the neutral and cationic nitrenes.

Although for formal electron counting purposes the complexes I–III are V(IV) complexes, they behave as reductants because of the electron-rich (19e) nature of the complex. This is evident in the calculated volume integrated charges (Table VIII) for Cp_2VNPh. The charge on V is greater than on N even though formal assignment of charge by electronegativities would have N in the −3 oxidation state and vanadium +4. Calculated charges suggest an electron-rich vanadium core with a slightly electron-deficient nitrene nitrogen. The preceding observations that the odd electron is localized on V and readily lost to generate a cationic V(V) species support this view.

Acknowledgment. This material is based on work supported by the Air Force Office of Scientific Research (AFOSR-84-0021

to W.C.T.), and W.C.T. thanks the Alfred P. Sloan Foundation for a research fellowship. Funds supporting the purchase of the University of Delaware diffractometer were provided by NSF.

Supplementary Material Available: Tables of observed and calculated structure factors, bond distances and angles, anisotropic temperature factors, hydrogen atom coordinates, and a charge analysis for all valence molecular orbitals from SCF–Xα–DV calculations (25 pages). Ordering information is given on any current masthead page.

Nucleophilic Attack on η^2-Acetyl Ligands. Structure of a Bridging η^2-Acetone Complex

Bruce D. Martin, Stephen A. Matchett, Jack R. Norton,* and Oren P. Anderson*

Contribution from the Department of Chemistry, Colorado State University, Fort Collins, Colorado 80523. *Received July 5, 1985*

Abstract: The formation of the acetyl/oxycarbene bridge in **3** from the η^2-acetyl complex **2** occurs by nucleophilic attack on the η^2-acetyl carbon by the Mo of the (μ-*OC*)Mo(CO)$_2$Cp ligand of **2**. Nucleophilic attack on the same carbon by the Zr–Me bond of Cp_2ZrMe_2 gives a trinuclear complex **4** with a bridging η^2-acetone. The crystal structure of **4c**, with η^5-C_5H_4Me ligands on Zr, has been determined by single-crystal X-ray diffraction methods and refined to an R (R_w) value of 0.037 (0.039) for 4429 reflections with $F_o > 5\sigma(F_o)$. The space group is $P2_1/c$, $Z = 4$, and the cell dimensions are $a = 8.683$ (2) Å, $b = 17.814$ (3) Å, $c = 21.852$ (6) Å, and $\beta = 93.53$ (2)°. The acetone of **4c** is η^2-*C,O* toward one Zr atom, and η^1-*O* toward the other Zr atom, with a C–O distance of 1.469 (5) Å.

In previous papers,[1] we have reported the characterization of the heterobimetallic complex **1**, its carbonylation to the η^2-acetyl complex **2**, and the decarbonylation of **2** to the acetyl/oxycarbene bridged **3**, an isomer of **1**. One possible mechanism for the

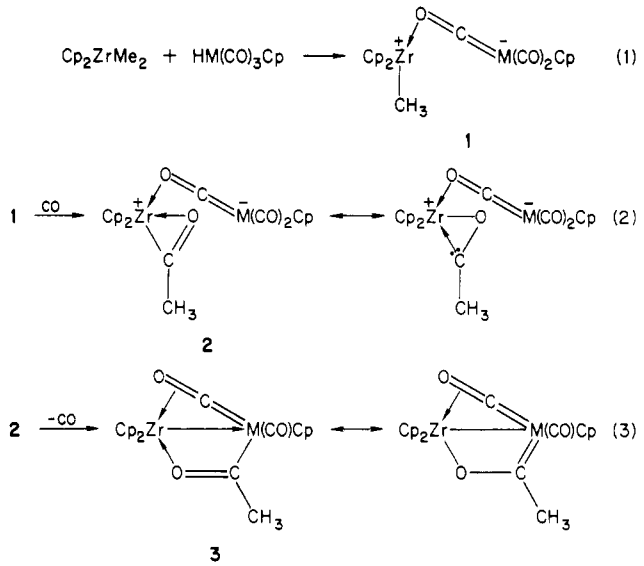

series a, CpM=(η^5-C_5H_5)Mo, Cp_2Zr=(η^5-C_5H_5)$_2$Zr
series b, CpM=(η^5-C_5H_4Me)Mo, Cp_2Zr=(η^5-C_5H_4Me)$_2$Zr
series c, CpM=(η^5-C_5H_5)Mo, Cp_2Zr=(η^5-C_5H_4Me)$_2$Zr
series d, CpM=(η^5-C_5H_5)W, Cp_2Zr=(η^5-C_5H_5)$_2$Zr

formation of **3** from **2** involved a carbene migration from the oxophilic zirconium onto the low-valent molybdenum. This mechanism, reaction 4, found precedent in the oxycarbene resonance structure invoked to explain other reactions of η^2-acetyl ligands, e.g., their dimerization through carbon.[2] We therefore

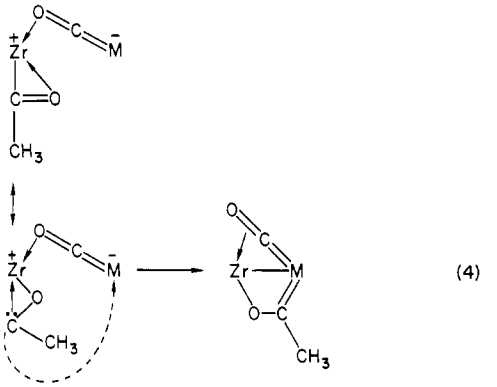

investigated the ability of η^2-acetyl ligands on $Cp_2Zr(IV)$ to serve as oxycarbene ligands toward other metals with accessible coordination sites. However, reactions 5–8 did not lead to the formation of an oxycarbene-bridged heterobimetallic; the reaction most commonly observed instead (e.g., reactions 5 and 6) was coordination of the carbon monoxide made available by slow decarbonylation of the η^2-acetyl.

We then hypothesized that reaction 3 might be better described as a *nucleophilic* attack by the molybdenum of the $CpMo(CO)_3^-$ fragment of **2** on the η^2-acetyl ligand carbon of **2**. We have therefore investigated the kinetics and mechanism of the conversion of **2** to **3** (reaction 3) and have discovered that the η^2-acetyl ligand of **2** is indeed subject to nucleophilic attack at carbon.

Results

Between 37.2 and 60.8 °C in toluene, reaction 3 proved first-order in [**2**] and independent of the CO pressure (up to 6.8 atm) and of the presence of added **3**. The reaction was roughly twice as fast in toluene as in THF. The temperature dependence

(1) (a) Longato, B.; Norton, J. R.; Huffman, J. C.; Marsella, J. A.; Caulton, K. G. *J. Am. Chem. Soc.* **1981**, *103*, 209. (b) Marsella, J. A.; Huffman, J. C.; Caulton, K. G.; Longato, B.; Norton, J. R. *J. Am. Chem. Soc.* **1982**, *104*, 6360. (c) Edidin, R. T.; Longato, B.; Martin, B. D.; Matchett, S. A.; Norton, J. R. In "Organometallic Compounds: Synthesis, Structure and Theory"; Shapiro, B. L., Ed.; Texas A&M University Press: College Station, TX, 1983; pp 260–280. (d) Longato, B.; Martin, B. D.; Norton, J. R.; Anderson, O. P. *Inorg. Chem.* **1985**, *24*, 1389.

(2) (a) Wolczanski, P. T.; Bercaw, J. E. *Acc. Chem. Res.* **1980**, *13*, 121 and references therein. (b) Threlkel, R. S.; Bercaw, J. E. *J. Am. Chem. Soc.* **1981**, *103*, 2650.

0002-7863/85/1507-7952$01.50/0